

Interplay between superconductivity and the Kondo effect on magnetic nanodots

Cite as: Appl. Phys. Lett. **118**, 152407 (2021); doi: [10.1063/5.0046108](https://doi.org/10.1063/5.0046108)

Submitted: 1 February 2021 · Accepted: 26 March 2021 ·

Published Online: 15 April 2021



View Online



Export Citation



CrossMark

Hyunsoo Yang,^{1,a)}  Mahn-Soo Choi,²  Grzegorz Ilnicki,³ Jan Martinek,³  See-Hun Yang,⁴  and Stuart Parkin^{4,a)}

AFFILIATIONS

¹Department of Electrical and Computer Engineering, National University of Singapore, 117576 Singapore

²Department of Physics, Korea University, Seoul 02841, South Korea

³Institute of Molecular Physics, Polish Academy of Sciences, Smoluchowskiego 17, 60-179 Poznan, Poland

⁴Max Planck Institute of Microstructure Physics, Weinberg 2, 06120 Halle, Germany

Note: This paper is part of the APL Special Collection on Mesoscopic Magnetic Systems: From Fundamental Properties to Devices.

a) Authors to whom correspondence should be addressed: eleyang@nus.edu.sg and stuart.parkin@mpi-halle.mpg.de

ABSTRACT

We study the interplay of superconductivity, ferromagnetism, and the Kondo effect in a single system, using vertical geometry and planar magnetic tunnel junction devices, in which a thin CoFe layer is inserted in the middle of the MgO layer, forming a quantum dot like system. It is shown that the Kondo resonance peak at the zero bias coexists with a sharp Bardeen-Cooper-Schrieffer gap on double tunnel junctions, Al/MgO/CoFe nanodot/MgO/Al. It is also found that the competition between superconductivity and the Kondo effect is tunable with magnetic fields and the temperature. The coexistence of Kondo screening and superconductivity survives long range magnetic order in CoFe nanodots with a spin polarization of 0.2; however, it disappears when the CoFe layer becomes a continuous film with a spin polarization of 0.5. The competition between SC and the Kondo effect in the presence of magnetic ordering opens exciting possibilities to control information in nanomagnets.

Published under license by AIP Publishing. <https://doi.org/10.1063/5.0046108>

The transport characteristics of spin-polarized carriers in magnetic nanostructures have long been of great interest. For example, the interaction of superconductivity (SC) and ferromagnetism (FM) has been studied by the proximity effect, when a ferromagnet is placed in contact with a superconductor.^{1,2} By the insertion of a tunnel barrier between the ferromagnet and the superconductor, spin-charge separation leads to the extremely long quasiparticle spin lifetimes.^{3,4} It is generally known that the Kondo effect cannot be found in ferromagnetically ordered systems, the Kondo effect competes with superconductivity (SC), and ferromagnetism (FM) tends to suppress both the Kondo effect and the SC. However, it has been shown recently that the Kondo effect can interact with either ferromagnetism or superconductivity, especially at the nanoscale, as reported from studies on interplay among SC, FM, and Kondo phenomena.^{5–8} In addition, Kondo systems have particularly attracted a great deal of attention since it was discovered from the Kondo insulator, SmB₆, that topological conductive states are formed on the surfaces, while the interior bulk is insulating.⁹

Typical tunneling Kondo experiments have been carried out through single electron transistors using artificial GaAs atoms¹⁰ and carbon nanotube quantum dots,¹¹ or break junctions with single molecular quantum dots.⁶ Kondo-assisted tunneling has also been

studied using the planar tunnel junctions doped with paramagnetic impurities, in which the zero-bias anomaly of the conductance around zero bias arises due to the Kondo resonance.^{12–14}

In this work, we study the triad interplay of SC-FM-Kondo and report that a Kondo zero-bias anomaly coexists with SC in the presence of the ferromagnetic nanodots using double tunnel junctions (DTJs), SC/insulator/FM/insulator/SC. It is found that the Kondo correlation can survive with a spin polarization of 0.2, whereas it is fully suppressed when the nanodots are sufficiently large to make a ferromagnetic state with a spin polarization of ~ 0.5 . We also provide a theoretical foundation to understand the exotic Kondo phenomena in superconducting-magnetic systems considering a finite spin polarization and multi-level quantum dots. Our experiments report the interplay of superconductivity and the Kondo effect in magnetic quantum dots, which brings a third phenomenon, namely, magnetism into the intriguing interplay between superconductivity and quantum dots. Our findings not only provide a rich platform to understand the exotic triad interplay of SC-FM-Kondo but also promote the development of new types of devices, in which the superconductivity can be controlled by Kondo interaction and magnetic information can be manipulated by the Kondo resonance.

We use a vertical geometry and planar magnetic tunnel junction (MTJ) device in Fig. 1(a) composed of Al superconducting electrodes and MgO tunnel barriers. Magnetic and superconducting tunnel junctions of the $700\ \mu\text{m} \times 700\ \mu\text{m}$ junction area were deposited on Si substrate/SiO₂ (25 nm) using high vacuum ($\sim 2 \times 10^{-9}$ Torr) dc magnetron sputtering at ambient temperature and were patterned using a sequence of *in situ* metal shadow masks. The junction structures without nanodots were 5 Al/3.4 MgO/6.5 Al (thicknesses in nm). Junctions with a nanodot layer were formed from 5.5 Al/2.5 MgO/0.75 Co₇₀Fe₃₀/2.5 MgO/6.5 Al (thicknesses in nm). MgO barriers are formed by reactive magnetron sputtering in an Ar–O₂ mixture.^{15,16} Conductance measurements were carried out in a ³He refrigerator using standard ac lock-in four-probe techniques.

A thin CoFe layer is inserted in the middle of the MgO layer, which forms a discontinuous layer of nanodots, as revealed by plan-view transmission electron microscopy (TEM) shown in Fig. 1(b). A clear ferromagnetic loop was measured from nanodot multilayers of the form [MgO/0.75 nm CoFe]₂₀ using a superconducting quantum interference device (SQUID) magnetometer at 5 K as shown in Fig. 1(c). Strong Coulomb repulsion on nanodots also suppresses the direct proximity effects, as demonstrated by the Cooper-pair splitter experiments.^{17,18} The competition between superconductivity and the Kondo effect can be determined by the relative strength $k_B T_K / \Delta$ of the Kondo temperature ($T_K \sim 20$ K) vs the superconducting gap energy ($\Delta = 0.35$ meV), where k_B is the Boltzmann constant, and can be tuned by the temperature and an external magnetic field. The energy level schematic diagram of a nanodot between two Al superconducting leads is shown in Fig. 1(d).

Due to a Coulomb blockade effect, as the temperature and bias voltage are reduced below 50 K and 27 meV, respectively, the dc

resistance of the Al/MgO/CoFe dot/MgO/Al MTJ increases rapidly as shown in Fig. 2(a) as similarly found in other reports.^{19–22} When the temperature further decreases below ~ 20 K, a peak centered at zero voltage in the tunneling conductance vs bias voltage curve appears as shown in Fig. 2(b). These features are due to the Kondo resonance previously observed in MTJs with magnetic and nonmagnetic electrodes, in which the temperature dependence of the conductance peak can be fitted to the empirical Kondo formula.^{20,23,24} Similar to other tunneling Kondo experiments, the conductance peak, observed in Fig. 2(b) around zero bias at low bias voltage and low temperatures, gradually disappears as the temperature increases. At lower temperatures, a double-peak structure is observed with a small splitting between them, which is in contrast to the observation of a single conductance peak for a single magnetic grain.²⁵

Figure 3(a) shows the conductance data from the Al/MgO/CoFe dot/MgO/Al junction, when the sample temperature is further reduced below the superconducting transition temperature of Al ($T_C \sim 2$ K). Clearly, two peaks at $\pm 2\Delta_{\text{Al}}$ are superimposed on a broad double conductance peak around zero bias. For reference, a sample without nanodots (Al/MgO/Al) in Fig. 3(e) does not show any broad conductance peak, in which negligible conductance within the gap and very sharp conductance peaks at $\Delta_1 + \Delta_2$, corresponding to the sum of the gap energies from the bottom (Δ_1) and top (Δ_2) superconducting electrodes, show that the junction is of good quality without any pinholes. Therefore, we can conclude that a broad double conductance peak is due to the Kondo resonance and two sharp peaks at $\pm 2\Delta_{\text{Al}}$ are from superconductivity of Al in Fig. 3(a).

Without the Kondo effect, the strong tunnel barriers and strong Coulomb repulsion suppress the transport through the quantum dot. However, once the Kondo effect arises, the Kondo resonance level is developed at the Fermi energy. This Kondo resonance level is effectively *non-interacting* although the bare level has strong Coulomb interaction. This Fermi-liquid picture of the Kondo resonance level has been well established.^{26,27} Therefore, the Cooper pairs in the superconducting electrodes can pass through the quantum dot via the Kondo resonance level. This is only possible due to the fact that in the Kondo regime, the system approaches the strong coupling limit and the conductance is much enhanced compared to the direct tunneling limit. The direct tunneling through two MgO barriers (total 5 nm thick) can be ruled out, as its contribution to the conductance ($0.68 \times 10^{-4} e^2/h$) would be 4 orders of magnitude smaller than that of higher order tunneling.²⁸ We report the interplay of superconductivity and the Kondo effect in magnetic nanodots, which brings a third effect (magnetism) to the intriguing interplay as we discuss later. Due to strong tunnel barriers and junction asymmetry, we do not observe the Josephson effect nor Andreev scattering processes in our samples. The finite subgap conductance in Figs. 3(a)–3(d) suggests that the devices are in the intermediate regime between the overdamped and underdamped regime. In the Kondo-mediated proximity effect, the induced gap is almost the same as that in the superconducting electrodes.^{29,30} For example, the sum of the gap energies of 1.448 mV in Fig. 3(b) is the same as that in Fig. 3(e). The asymmetric bias voltage dependence of the conductance in Figs. 3(a) and 3(c) is attributed to the difference in the capacitances and resistances over the two tunnel barriers, which is typical for asymmetric junction geometry.⁶ Thermally excited quasiparticles featured as a peak at zero bias substantiate the existence of superconductivity at the elevated temperature

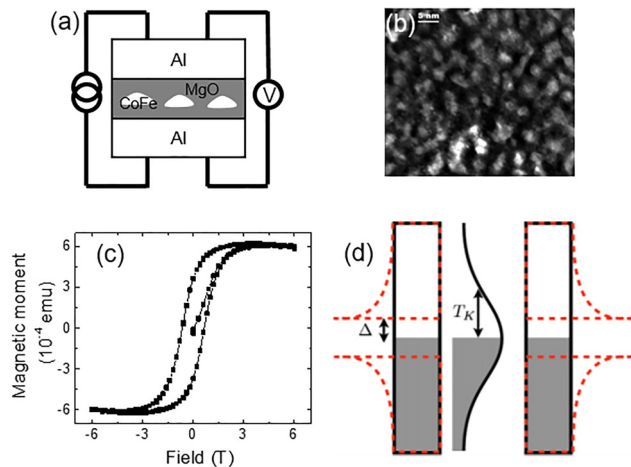


FIG. 1. (a) Diagram showing the measurement geometry, in which a discontinuous layer of CoFe nanodots is inserted in the middle of the MgO tunnel barrier. (b) A plane view TEM image when a nominal thickness 0.75 nm CoFe layer is deposited. Black color represents MgO, and white regions correspond to CoFe nanodots. (c) Magnetization vs magnetic field curve of the form [MgO/0.75 nm CoFe]₂₀ at 5 K showing that the CoFe nanodots have a long range magnetic ordering. (d) Schematic energy diagram in the regime $k_B T_K > \Delta$ showing a resonance state of a dot with Al superconducting electrodes. Δ is the superconducting gap and the Kondo temperature T_K is proportional to the width of the resonance level.

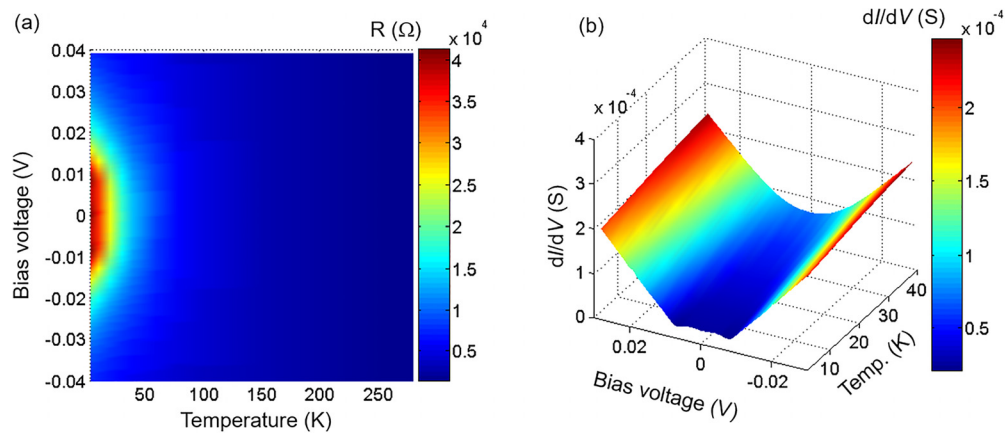


FIG. 2. DC resistance (a) and conductance (b) of an MTJ with a structure of Al/MgO/CoFe dot/MgO/Al. A magnetic field of 1 T was applied to an MTJ. Due to a Coulomb blockade effect, the junction resistance in (a) increases at a greater rate, when the temperature is reduced below 50 K or the bias voltage is smaller than 27 mV. The conductance peak is observed in (b) around zero bias at low bias voltage and low temperatures, which gradually disappear as the temperature increases.

of 1.4 K as shown in Figs. 3(d) and 3(f) for the samples with and without nanodots, respectively.³¹

The magnetization curve of Fig. 1(c) implies that CoFe nanodots have a large macroscopic magnetic moment. However, as elaborated theoretically and demonstrated experimentally, ferromagnetism itself does not necessarily destroy the Kondo effect.^{6,32–34} The transport phenomenon is governed only by the states near the Fermi energy of the magnetic dot, and the spin-polarized electrons far below the Fermi level contribute only to the magnetization but not to the transport. The most crucial factor is, thus, the spin polarization (P) at the Fermi surface.^{6,32–34} The spin polarization at the Fermi level of CoFe nanodots is estimated to be 0.2,^{20,35,36} and it turns out that the Kondo correlation can survive with a spin polarization of 0.2 as we show below.

We examine the effects of the spin polarization in the magnetic nanodot on the Kondo correlation. The s -band in CoFe nanodots is quantized into discrete levels due to spatial confinement. The average level spacing is estimated to be 0.3–1 meV for nanodots of diameter 3.2 nm. In order to focus on the effects of a finite spin polarization, $P = (\Gamma_{\uparrow} - \Gamma_{\downarrow}) / (\Gamma_{\uparrow} + \Gamma_{\downarrow}) = 0.2$, we assume three spin up quantized levels and two spin down levels in the nanodot, all with the same energy ε_d . This simplified picture of the magnetic nanodot is described by the following Anderson-like Hamiltonian equation:

$$H_D = \sum_{\sigma=\uparrow,\downarrow} \sum_{j=1}^{g_{\sigma}} \varepsilon_d d_{j\sigma}^{\dagger} d_{j\sigma} + \frac{1}{2} U n(n-1), \quad (1)$$

where U is the interaction energy of the order of the Coulomb charging energy E_c and $n = \sum_{\sigma} \sum_j^{g_{\sigma}} d_{j\sigma}^{\dagger} d_{j\sigma}$ is the total number of electrons occupying the dot levels. In Eq. (1), the spin polarization is effectively manifested by the spin-dependent degeneracy factor g_{σ} (we have assumed $g_{\uparrow} = 3$ and $g_{\downarrow} = 2$).

If the magnetic nanodot is coupled to a (spin-unpolarized) conduction band of an electrode, the total Hamiltonian takes the form $H = H_C + H_D + H_T$, where $H_C = \sum_{k\sigma} \varepsilon_k c_{k\sigma}^{\dagger} c_{k\sigma}$ describes the conduction band and $H_T = t \sum_{k\sigma} \sum_j (c_{k\sigma}^{\dagger} d_{j\sigma} + d_{j\sigma}^{\dagger} c_{k\sigma})$ is responsible for the tunneling between the dot and the conduction band, where we have assumed energy-independent tunneling amplitude t .

If we change the basis and define new operators $a_{0\uparrow} = \frac{d_{1\uparrow} + d_{2\uparrow} + d_{3\uparrow}}{\sqrt{3}}$, $a_{1\uparrow} = \frac{d_{1\uparrow} + d_{2\uparrow} - 2d_{3\uparrow}}{\sqrt{3}}$, $a_{2\uparrow} = \frac{d_{1\uparrow} - d_{2\uparrow}}{\sqrt{2}}$, $a_{0\downarrow} = \frac{d_{1\downarrow} + d_{2\downarrow}}{\sqrt{2}}$, $a_{1\downarrow} = \frac{d_{1\downarrow} - d_{2\downarrow}}{\sqrt{2}}$, H_T becomes $H_T = \sum_k [\sqrt{3}t(c_{k\uparrow}^{\dagger} a_{0\uparrow} + a_{0\uparrow}^{\dagger} c_{k\uparrow}) + \sqrt{2}t(c_{k\downarrow}^{\dagger} a_{0\downarrow} + a_{0\downarrow}^{\dagger} c_{k\downarrow})]$. Only $a_{0\sigma}$ electrons are tunnel-coupled to the conduction band with $a_{1\uparrow}$, $a_{2\uparrow}$, $a_{1\downarrow}$ all decoupled (the latter are still coupled through the U -term in H_D , but the effect is negligible). The crucial point is that the tunneling amplitudes $\sqrt{3}t$ and $\sqrt{2}t$ for $a_{0\uparrow}$ and $a_{0\downarrow}$, respectively, are different from each other. Let $\Gamma_{\uparrow} = 3\Gamma_0$, $\Gamma_{\downarrow} = 2\Gamma_0$, $\Gamma_0 = \pi|t|^2 N_0$, with N_0 being the density of states of the conduction band at the Fermi level. Then, the model is equivalent to a non-magnetic quantum dot coupled to ferromagnetic leads with (parallel) polarization,^{32,34} $P = 0.2$.

As in a quantum dot coupled to ferromagnetic leads, the Kondo temperature depends on the polarization³² given by $T_K(P) = \sqrt{\frac{(\Gamma_{\uparrow} + \Gamma_{\downarrow})U}{4}} \exp\left[\frac{\pi\varepsilon_d}{\Gamma_{\uparrow} + \Gamma_{\downarrow}} \left(1 + \frac{\varepsilon_d}{U}\right) \frac{\tanh^{-1}(P)}{P}\right]$. A finite polarization P tends to suppress the Kondo temperature T_K . However, in our case, the spin polarization ($P = 0.2$) is rather small, and its effect is relatively small compared with the multilevel effects. While the polarization increases the (negative) exponent by a factor of 1.014, the multilevel effect decreases it by a factor of 2/5. This can explain the high Kondo temperature observed in our experiment even in the presence of a finite spin polarization.

Controlling the spin polarization value provides an opportunity to control the strength of the Kondo effect and the superconductivity. For example, Kondo features are fully suppressed when the CoFe nanodot layer is thickened to make a continuous ferromagnetic layer, in which the spin polarization is ~ 0.5 .^{20,23} Figure 4(a) shows the conductance from an MTJ with a 2 nm CoFe layer in the middle of the structure (Al/MgO/2 nm CoFe film/MgO/Al), which does not show any conductance peak or double-peaked structure, as a strong magnetic ordering completely suppresses the Kondo effect. We, thus, identify the unpaired electrons on the nanodots to be responsible for the Kondo effect. The mechanism of our Kondo effect is distinguished from that in the Co adatom on a metal surface, in which the 4s electrons of Co are strongly and chemically hybridized with host metals and one of the d orbitals is involved in the Kondo effect.²⁵ The average

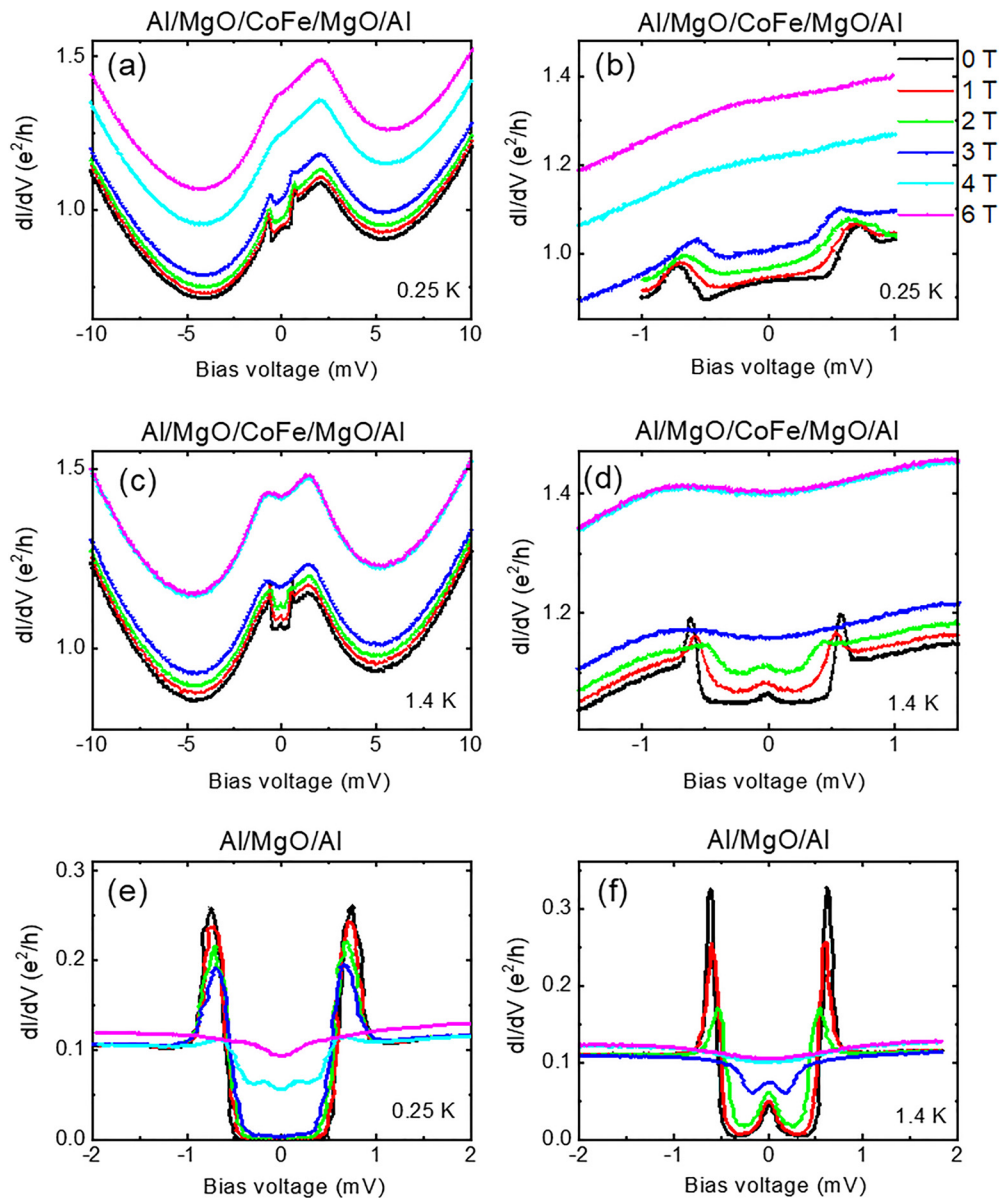


FIG. 3. Conductance data for an MTJ device of Al/2.5 nm MgO/CoFe dot/2.5 nm MgO/Al for a wide [(a) and (c)] and narrow [(b) and (d)] range of bias voltages at 0.25 K and 1.4 K, respectively. Two clear superconducting gap peaks at $\pm 2\Delta_{\text{Al}}$ superimpose a broad Kondo conductance peak around zero bias. [(e) and (f)] Conductance data for an MTJ device without a nanodot layer (Al/3.4 nm MgO/Al) at 0.25 K and 1.4 K. At 1.4 K, thermally excited quasiparticles lead to an additional peak at zero bias in (d) and (f). The legend in (b) indicates the applied magnetic field.

discrete level spacing in CoFe nanodots is estimated to be 0.3–1 meV from the mean diameter (~ 3.2 nm).^{19,37} The tunneling broadening $\Gamma \sim 3$ meV is consistent with other results.²³ The level spacing is, thus, likely to be smaller than or comparable to at most the tunnel broadening. It is known that the Kondo temperature can be enhanced by several orders of magnitude in multi-level quantum dots,^{38–40} which can explain the observed strong Kondo phenomena in magnetic systems.

The Kondo-mediated proximity effect has been demonstrated previously in three different types of experiments. The first one is the

conductance characteristics through an SC/dot/SC junction,^{7,11,41–44} which is consistent with Fig. 3. The second example is a direct measurement of supercurrent, which usually involves interferometry.^{8,45} The third case is a probe of the local density of states (LDOS) by means of the conductance in FM/dot/SC junctions.⁴⁶ In the last type of device, the Kondo-mediated proximity effect is induced by the superconducting electrode, and the ferromagnetic electrode probes the LDOS on the dot. In this sense, the ferromagnetic electrode plays a role of a scanning tunneling microscope tip. Figure 4(b) shows the

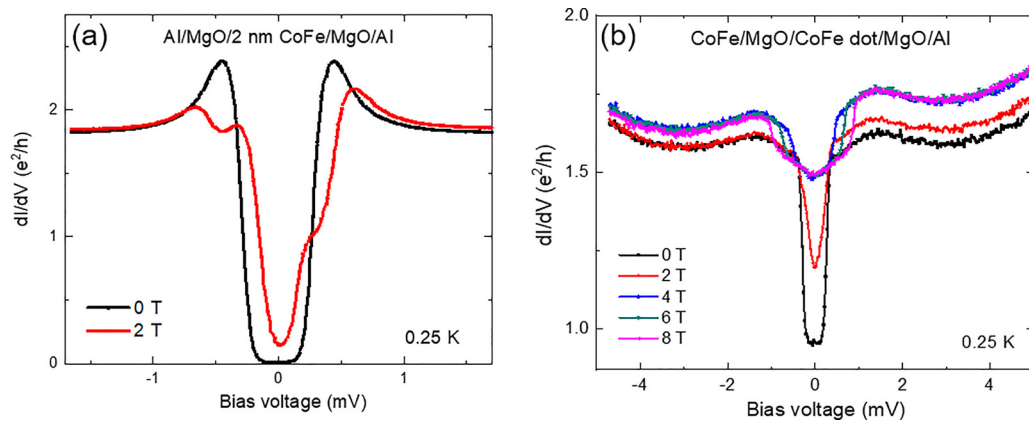


FIG. 4. (a) Conductance data for an MTJ device of Al/MgO/2 nm CoFe/MgO/Al. The Kondo resonance peak disappears due to a strong magnetic ordering in the continuous 2 nm CoFe layer. (b) Conductance data for an MTJ device of CoFe/MgO/CoFe dot/MgO/Al. The Kondo double-peaked behavior survives in an asymmetric structure with FM and SC contacts.

conductance characteristics on our FM/MgO/dot/MgO/SC device, which falls into this type of devices as recounted below in more detail.

It exhibits a conductance enhancement in the bias range of $0.35 < |V| < 2.5$ meV, which can be attributed to the Kondo resonance peak in the LDOS on the dot. As the bias voltage decreases further, the conductance is eventually suppressed in the range of $|V| < 0.35$ meV. The same suppression exactly in the same bias range is observed in an FM/(continuous film)/SC device (i.e., *without dot*) as illustrated in Fig. 4(a) at 0 T. Considering the superconducting gap $\Delta = 0.35$ meV, it is clear that this suppression is due to the proximity-induced superconductivity on the dot, which suppresses the LDOS below the superconducting gap. On applying 2 T in Fig. 4(a), the superconducting tunneling spectroscopy data mimic that of a ferromagnetic-insulator-superconductor tunnel junction with a tunneling spin polarization of ~ 0.5 due to a continuous CoFe thin film.⁴⁷ Figure 4(b), thus, demonstrates clearly that the Kondo-mediated proximity effect indeed survives even in the presence of the magnetic ordering on the nanodot. A step in the conductance in Fig. 4(b) shifts to a higher bias voltage by $g\mu_B B$ upon increasing the magnetic field (B) from 4 to 8 T, where μ_B is the Bohr magneton and g factor (g) is 2. This characteristic step corresponds to the voltage at which an inelastic spin-flip cotunneling process is activated.²³

In summary, we have studied the magneto-transport in double tunnel junctions (Al/MgO/CoFe nanodot/MgO/Al). A clear superconductivity feature superimposed on top of the broad conductance enhancement due to the Kondo effect is observed. The measured conductance data show the competition between superconductivity and the Kondo effect in the presence of ferromagnetic nanodots depending on magnetic fields and the temperature. The Kondo correlation can survive with a spin polarization of 0.2, whereas Kondo features are fully suppressed with the spin polarization of ~ 0.5 . Our findings demonstrate that a superconducting tunnel junction with magnetic nanodots serves as a rich platform to understand the interplay of superconductivity, ferromagnetism, and the Kondo effect and to explore superconductor-based spin devices.

This research was partly supported by the National Science Centre, Poland, Grant Nos. 2015/17/B/ST3/02799 and 2020/36/C/

ST3/00539. M.-S.C. was supported by the National Research Foundation of Korea (Grant Nos. 2018R1A4A1024157 and 2017R1E1A1A03070681) and the Ministry of Education of Korea (BK21 Four).

DATA AVAILABILITY

The data that support the findings of this study are available from the corresponding author upon reasonable request.

REFERENCES

- ¹T. Kontos, M. Aprili, J. Lesueur, and X. Grison, *Phys. Rev. Lett.* **86**, 304 (2001).
- ²F. S. Bergeret, A. F. Volkov, and K. B. Efetov, *Phys. Rev. Lett.* **86**, 4096 (2001).
- ³H. Yang, S.-H. Yang, S. Takahashi, S. Maekawa, and S. S. P. Parkin, *Nat. Mater.* **9**, 586 (2010).
- ⁴S. Takahashi, H. Imamura, and S. Maekawa, *Phys. Rev. Lett.* **82**, 3911 (1999).
- ⁵M. R. Calvo, J. Fernandez-Rossier, J. J. Palacios, D. Jacob, D. Natelson, and C. Untiedt, *Nature* **458**, 1150 (2009).
- ⁶A. N. Pasupathy, R. C. Bialczak, J. Martinek, J. E. Grose, L. A. K. Donev, P. L. McEuen, and D. C. Ralph, *Science* **306**, 86 (2004).
- ⁷K. J. Franke, G. Schulze, and J. I. Pascual, *Science* **332**, 940 (2011).
- ⁸J. P. Cleuziou, W. Wernsdorfer, V. Bouchiat, T. Ondarcuhu, and M. Monthieux, *Nat. Nanotechnol.* **1**, 53 (2006).
- ⁹K. S. Lu Li, C. Kurdak, and J. W. Allen, *Nat. Rev. Phys.* **2**, 463 (2020).
- ¹⁰D. Goldhaber-Gordon, H. Shtrikman, D. Mahalu, D. Abusch-Magder, U. Meirav, and M. A. Kastner, *Nature* **391**, 156 (1998).
- ¹¹M. R. Buitelaar, T. Nussbaumer, and C. Schönenberger, *Phys. Rev. Lett.* **89**, 256801 (2002).
- ¹²L. Y. L. Shen and J. M. Rowell, *Phys. Rev.* **165**, 566 (1968).
- ¹³J. Appelbaum, *Phys. Rev. Lett.* **17**, 91 (1966).
- ¹⁴E. L. Wolf, *Principles of Electron Tunneling Spectroscopy* (Oxford University Press, New York, 1989).
- ¹⁵S. S. P. Parkin, C. Kaiser, A. Panchula, P. Rice, B. Hughes, M. Samant, and S.-H. Yang, *Nat. Mater.* **3**, 862 (2004).
- ¹⁶H. Yang, S.-H. Yang, and S. Parkin, *AIP Adv.* **2**, 012150 (2012).
- ¹⁷L. Hofstetter, S. Csonka, J. Nygard, and C. Schönenberger, *Nature* **461**, 960 (2009).
- ¹⁸L. G. Herrmann, F. Portier, P. Roche, A. L. Yeyati, T. Kontos, and C. Strunk, *Phys. Rev. Lett.* **104**, 026801 (2010).
- ¹⁹K. Yakushiji, F. Ernult, H. Imamura, K. Yamane, S. Mitani, K. Takahashi, S. Maekawa, and H. Fujimori, *Nat. Mater.* **4**, 57 (2004).
- ²⁰H. Yang, S. Yang, and S. Parkin, *Nano Lett.* **8**, 340 (2008).

- ²¹L. F. Schelp, A. Fert, F. Fetta, P. Holody, S. F. Lee, J. L. Maurice, F. Petroff, and A. Vaur, *Phys. Rev. B* **56**, R5747 (1997).
- ²²H. Sukegawa, S. Nakamura, A. Hirohata, N. Tezuka, and K. Inomata, *Phys. Rev. Lett.* **94**, 068304 (2005).
- ²³H. Yang, S.-H. Yang, G. Ilnicki, J. Martinek, and S. S. P. Parkin, *Phys. Rev. B* **83**, 174437 (2011).
- ²⁴D. Goldhaber-Gordon, J. Göres, M. A. Kastner, H. Shtrikman, D. Mahalu, and U. Meirav, *Phys. Rev. Lett.* **81**, 5225 (1998).
- ²⁵T. W. Odom, J.-L. Huang, C. L. Cheung, and C. M. Lieber, *Science* **290**, 1549 (2000).
- ²⁶L. I. Glazman and K. A. Matveev, *JETP Lett.* **49**, 659 (1989).
- ²⁷P. Nozières, *J. Low Temp. Phys.* **17**, 31 (1974).
- ²⁸S. Yuasa, T. Nagahama, A. Fukushima, Y. Suzuki, and K. Ando, *Nat. Mater.* **3**, 868 (2004).
- ²⁹A. F. Volkov, P. H. C. Magnée, B. J. van Wees, and T. M. Klapwijk, *Physica C* **242**, 261 (1995).
- ³⁰C. W. J. Beenakker and H. van Houten, *Single-Electron Tunneling and Mesoscopic Devices* (Springer, 1992), Vol. 31.
- ³¹R. Meservey and P. M. Tedrow, *Phys. Rep.* **238**, 173 (1994).
- ³²J. Martinek, Y. Utsumi, H. Imamura, J. Barnas, S. Maekawa, J. König, and G. Schön, *Phys. Rev. Lett.* **91**, 127203 (2003).
- ³³M.-S. Choi, N. Y. Hwang, and S. R. Eric Yang, *Phys. Rev. B* **67**, 245323 (2003).
- ³⁴M.-S. Choi, D. Sanchez, and R. Lopez, *Phys. Rev. Lett.* **92**, 056601 (2004).
- ³⁵H. Yang, S.-H. Yang, C. Kaiser, and S. Parkin, *Appl. Phys. Lett.* **88**, 182501 (2006).
- ³⁶R. J. Soulen, J. M. Byers, M. S. Osofsky, B. Nadgorny, T. Ambrose, S. F. Cheng, P. R. Broussard, C. T. Tanaka, J. Nowak, J. S. Moodera, A. Barry, and J. M. D. Coey, *Science* **282**, 85 (1998).
- ³⁷L. Y. Zhang, C. Y. Wang, Y. G. Wei, X. Y. Liu, and D. Davidovic, *Phys. Rev. B* **72**, 155445 (2005).
- ³⁸T. Inoshita, A. Shimizu, Y. Kuramoto, and H. Sakaki, *Phys. Rev. B* **48**, 14725 (1993).
- ³⁹M.-S. Choi, R. López, and R. Aguado, *Phys. Rev. Lett.* **95**, 067204 (2005).
- ⁴⁰J. S. Lim, M.-S. Choi, M. Y. Choi, R. López, and R. Aguado, *Phys. Rev. B* **74**, 205119 (2006).
- ⁴¹M. R. Buitelaar, W. Belzig, T. Nussbaumer, B. Babić, C. Bruder, and C. Schönberger, *Phys. Rev. Lett.* **91**, 057005 (2003).
- ⁴²C. Buizert, A. Oiwa, K. Shibata, K. Hirakawa, and S. Tarucha, *Phys. Rev. Lett.* **99**, 136806 (2007).
- ⁴³A. Eichler, M. Weiss, S. Oberholzer, C. Schönberger, A. L. Yeyati, J. C. Cuevas, and A. Martín-Rodero, *Phys. Rev. Lett.* **99**, 126602 (2007).
- ⁴⁴K. Grove-Rasmussen, H. I. Jørgensen, and P. E. Lindelof, *New J. Phys.* **9**, 124 (2007).
- ⁴⁵J. D. Pillet, C. H. L. Quay, P. Morfin, C. Bena, A. L. Yeyati, and P. Joyez, *Nat. Phys.* **6**, 965 (2010).
- ⁴⁶L. Hofstetter, A. Geresdi, M. Aagesen, J. Nygård, C. Schönberger, and S. Csonka, *Phys. Rev. Lett.* **104**, 246804 (2010).
- ⁴⁷H. Yang, S.-H. Yang, and S. S. P. Parkin, *Appl. Phys. Lett.* **90**, 202502 (2007).